Proceedings of the 2003 IEEE International Frequency Control Symposium and PDA Exhibition
Jointly with the 17th European Frequency and Time Forum

The Physics of Miniature Atomic Clocks: 0-0 versus "End" Resonances

Y-Y. Jau[(1)], A. B. Post[(1)], N. N. Kuzma[(1)], A. M. Braun[(2)], M. V. Romalis[(1)], W. Happer[(1)]
[1] Department of Physics, Princeton University, Princeton, NJ 08544 USA
[2] Sarnoff Corporation, Princeton, NJ 08543 USA

***Abstract*- We consider advantages of the "end" resonances for the minituarized alkali vapor-cell atomic clock, namely a higher signal-to-noise ratio (SNR) and a narrower linewidth at high vapor densities. We report our preliminary observations of the unusual phenomenon of light narrowing, in which the rubidium end-resonance linewidth is substantially reduced and the SNR greatly improved as the laser light intensity is increased. Contributions to the total linewidth from other broadening mechanisms are discussed.**

I. INTRODUCTION

The development of miniature atomic clocks [1] has a promising potential for mobile jam-resistant GPS receivers and high security UHF communication. For traditional alkali vapor-cell atomic clocks, spin-exchange collisions are the main contribution to the resonance linewidth [2]. This broadening mechanism is more severe in miniature cells, where alkali-metal number densities must be increased to obtain an adequate signal from the cell over a shorter optical-path length. The spin-exchange broadens the linewidth, reduces the signal-to-noise ratio and hence increases the uncertainty of the traditional clock resonance.

The clock resonance is based on the hyperfine splitting of stable alkali-metal isotopes, such as ^{133}Cs or ^{87}Rb. The vapor cells in atomic clocks are filled with alkali metal and a buffer gas, such as Ne, Ar, or N_2. At a given temperature some alkali atoms are in a vapor phase. A laser tuned to the D1 line is used to selectively excite the atoms from one of the two ground-state F multiplets, where $F=I\pm1/2$ is the total angular momentum of the alkali atom in units of $\hbar$, and I is the nuclear spin quantum number. A population imbalance is achieved between the two $I\pm1/2$ hyperfine multiplets. Microwave radiation, tuned to the multiplet splitting frequency, generates a coherent superposition state, generally between the two field-independent sublevels with the azimuthal angular momentum quantum number $m_F = 0$, shown in Fig. 1. This is the traditional 0-0 clock resonance.

The parameter

$$\sigma_\nu \propto \frac{1}{SNR}\cdot\frac{\Delta\nu}{\nu_{hf}} \qquad (1)$$

has traditionally been used [3] to measure the frequency uncertainty of an atomic clock controlled by a resonance of signal-to-noise ratio SNR and linewidth $\Delta\nu$. The high density alkali-metal vapor needed to compensate for the small cell size broadens the linewidth and decreases the signal-to-noise ratio of the 0-0 resonance. So both the numerator and denominator of (1) are degraded in small clocks. The end resonances are much more suitable for high temperature operation. Spin-exchange collisions conserve the total spin of the colliding pair of alkali-metal atoms. For the traditional 0-0 resonance, the colliding atoms have zero time-averaged spin. There are $2(2I+1)$ final states to which the collisions can transfer the atoms, so spin exchange collisions effectively interrupt the coherent oscillations and broaden the width of the 0-0 resonance line. Colliding atoms in the spin states for the end resonance have maximum (or minimum) spin angular momentum. There are few final states of the same high angular momentum to which they can be transferred. Therefore spin-exchange collisions cause little broadening of the end resonances. Pumping with circularly polarized D1 light places most of the atoms in the high spin states needed for the end resonances, ensuring that nearly all of the atoms participate. This substantially increases the SNR of the end resonance. There is no simple way to pump all of the atoms into the two sublevels needed for the traditional 0-0 resonance, so only a small fraction of the atoms can participate.

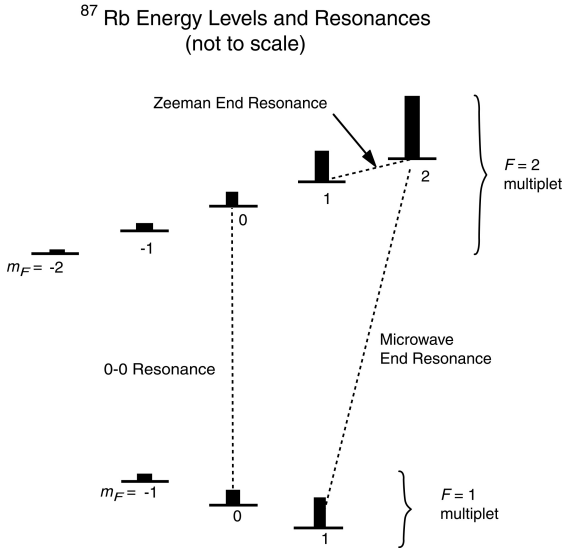

Figure 1. The ground state hyperfine levels of ^{87}Rb with $I = 3/2$.

The 0-0 resonance has a frequency shift that is proportional to the square of the ambient magnetic field. The coefficient of the shift is small enough that it is possible to operate 0-0 clocks with modest control of the magnetic field. The end resonance has a frequency shift directly proportional to the magnetic field, and the coefficient of the shift is large enough that active control of the field is necessary. By locking the local oscillator frequency and the magnetic field to both the microwave and Zeeman end resonances, it is possible to obtain excellent clock stability.

In the following sections, we discuss experiments that demonstrate the narrow linewidths and high SNR of the end resonances. We present data validating these two unique features of end resonances. Our data was obtained with cells containing isotopically enriched ^{87}Rb and N_2 buffer gas. Because of its lower nuclear spin I=3/2, ^{87}Rb has fewer hyperfine sublevels than both ^{85}Rb (I=5/2) and ^{133}Cs (I=9/2), but the physics discussed below can be easily extended to all half-integer spin isotopes.

II. Resonance Linewidth Prediction

There are five dominant contributions to the linewidth: optical pumping [4] of the Rb atoms with a photon flux Φ and a photon absorption cross section σ adds a contribution of order $\sigma\Phi$ [4]; spin-exchange collisions between pairs of Rb atoms of number density [Rb] make a contribution [2] to the linewidth on the order of the spin-exchange rate, κ_{ex}[Rb]; spin-rotation interactions [4] during collisions with nitrogen molecules of number density [N_2] will contribute to the linewidth on the order of the S-damping rate κ_{sd}[N_2]; the modification of the hyperfine splitting [5] during collisions with the nitrogen molecultes will make a contribution to the linewidth on the order of the Carver rate κ_C[N_2]. Recent experimental measurements of the rate coefficients κ_{ex} , κ_{sd} and κ_C can be found in [5]. The final contribution is D_0/l^2[N_2], the spin-diffusion rate [6] which determines the rate at which the atoms relax on the cell walls. The relation between the linewidth and the five contributions is summarized as following for the 0-0 and end transitions:

$$\Delta\nu_{0-0} = \pi^{-1}\left[\tfrac{3}{4}\sigma\Phi + \tfrac{5}{8}\kappa_{ex}[\mathrm{Rb}] + \tfrac{3}{4}\kappa_{sd}[\mathrm{N_2}] + 1.7\kappa_c[\mathrm{N_2}] + \frac{D_0}{\ell^2[\mathrm{N_2}]}\right] \quad (2)$$

$$\Delta\nu_{1-2} \approx \pi^{-1}\left[\tfrac{3}{4}\sigma\Phi + \kappa_{ex}[\mathrm{Rb}]\cdot f(\mathrm{P}) + \tfrac{7}{8}\kappa_{sd}[\mathrm{N_2}] + 1.7\kappa_c[\mathrm{N_2}] + \frac{D_0}{\ell^2[\mathrm{N_2}]}\right], \quad (3)$$

where the function $f(P)$ is defined as:

$$f(P) = \frac{(1-P)(11+5P^2)}{16(1+P^2)} \quad (4)$$

and the spin polarization P of ^{87}Rb atoms is

$$P = 2\langle S_z\rangle = \sigma\Phi\cdot\left[\sigma\Phi + \kappa_{sd}[\mathrm{N_2}] + D_0/(\ell^2[\mathrm{N_2}])\right]^{-1}. \quad (5)$$

Here $\langle S_z\rangle$ is the average electron spin value. The function $f(P)$ goes to zero as P goes to 1. One can see from (2)–(5) that in the case of complete polarization P=1, the spin-exchange rate makes no contribution to the end resonance linewidth. The linewidths predicted by (2)–(5) are plotted in Fig. 2. The downward slope of the end resonance curve (solid line) denotes the region of "light narrowing," which is due to the suppression of spin-exchange broadening at high polarization. The light narrowing is most pronounced when the linewidth is dominated by spin-exchange collisions. These are the conditions of miniature atomic clocks, where large densities of alkali-metal atoms are needed to compensate for the short path lengths of light through the vapor. The high densities of alkali-metal atoms are obtained by increasing the cell temperature. As Fig. 2 also demonstrates, the light narrowing is followed by a gradual light broadening as the light intensity continues to increase. The phenomenon described in this paper is similar to the light narrowing of the Zeeman end resonances (those between the states within the same F multiplet, as in Fig. 1) observed in Rb vapor by Appelt *et al.* [7].

In Fig. 3 we show the dependence of the end-resonance linewidth on the buffer gas density predicted by (2)–(3).

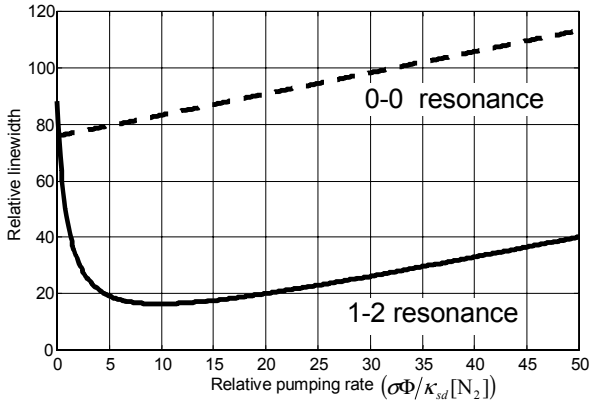

Figure 2. The calculation shows how the linewidths of the two resonances compare at high spin-exchange rates.

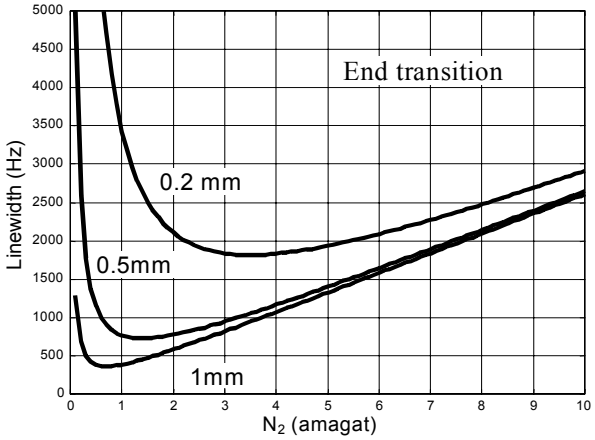

Figure 3. Calculation of linewidth dependence on the buffer gas pressure (1 amagat = 2.69×10^{19}cm^{-3}). The numbers on the plot denote cell thickness.

Increasing the buffer gas density [N_2] diminishes the linewidth contribution from diffusion to the cell walls, but it increases the collisional contribution from the spin-rotation and hyperfine pressure shift interactions.

III. Experimental Results

The experimental setup is shown in Fig. 4. The vapor cell is mounted inside the air-heated oven. The oven temperature is controlled by a thermal-sensor feedback loop. The laser beam is generated by a scanning Ti:Sapphire ring laser and is coupled to the system via an optical fiber. The laser intensity is adjusted with neutral density (ND) filters and the circular polarization is obtained using a polarizing beam splitter and a quarter-wave plate. The cell (1 to 2 mm optical thickness) is also irradiated by a microwave field from a horn. The microwave field is switched on and off at a low frequency of 50 Hz. There are three sets of Helmholtz coil pairs for compensating the ambient field and for producing the B_z field. By scanning the microwave frequency and using a lock-in amplifier, the resonance signal is obtained and then recorded by the computer.

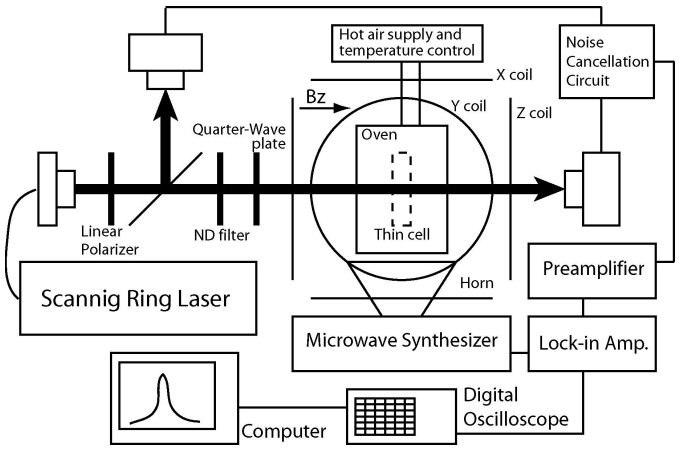

Figure 4. Experimental apparatus.

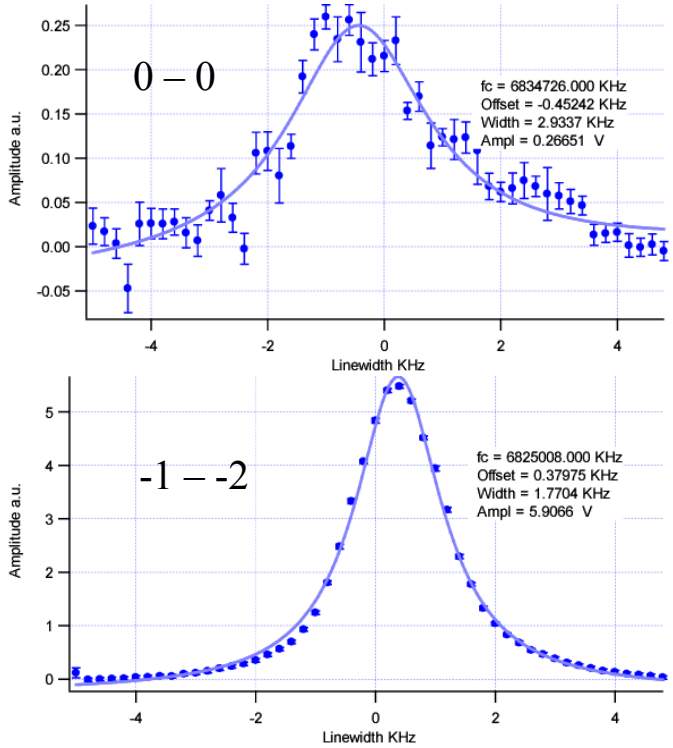

Figure 5. Two resonance signals at 95^{0}C from a cell filled (at room temperature) with ^{87}Rb and 80 torr of N_2 (circles with error bars), fitted to Lorentzians (smooth curves). At the same laser intensity and microwave power, the end resonance signal (bottom panel) shows lower linewidth, better contrast and higher SNR compared to the 0-0 resonance (top panel).

The data in Fig. 5 shows the striking difference observed experimentally between the two resonances: the end resonance has a narrower linewidth and a much better SNR compared to its 0-0 counterpart under the same temperature, laser and microwave power. At high temperatures the spin-exchange rate dominates the line broadening unless there are no allowed states to exchange with, as is the case for the end resonance at a high spin polarization.

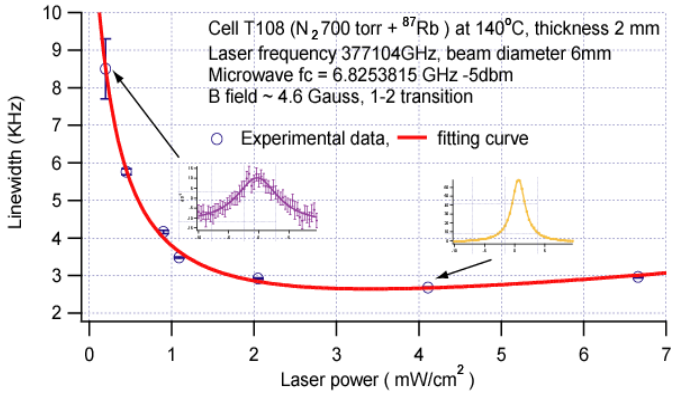

Figure 6. Increasing the laser intensity enhances the 1-2 end resonance's SNR and narrows its linewidth. Our experimental data is in a good agreement with the theoretical curve based on (2)–(5). The insets show experimental traces similar to those in Fig. 5.

Fig. 6 shows an experimental validation of the light narrowing prediction given in Fig. 2. The data were obtained using a 2 mm-thick cell filled (at room temperature) with about 0.9 atm of nitrogen gas. Nitrogen buffer gas was essential to quench the fluorescence of the excited atoms, thereby avoiding the depolarization caused by radiation trapping. As Fig. 6 demonstrates, our data fits well to the theoretical curves. At these temperatures and pressures, the 0-0 resonance signal disappears because of high spin-exchange rates and unresolved hyperfine levels.

IV. Conclusions and Further Work

This paper has summarized advantages of considering the end transitions for an atomic clock timebase instead of the

traditional 0-0 resonances. We have no reports of long term stability or accuracy, as we have yet to construct a functional clock in our laboratory. The reported experimental results are based on a resonance signal induced by a microwave source. We will proceed to detect the resonance signal by using an intensity modulated laser beam to both excite and probe the resonance. The advantages of using the end resonance in such system are expected to be the same as those reported here.

ACKNOWLEDGMENTS

We are grateful to many people for their help in this work. We are especially thankful to Mr. Mike Souza at the Chemistry Department of Princeton University, who made all the cells for our experiments. We are also thankful to Prof. Jacques Vanier for discussions.

This work was supported by the Air Force Office of Scientific Research (AFOSR) and the Defense Advanced Research Project Agency (DARPA).

REFERENCES

[1] J. Kitching, L. Hollberg, S. Knappe, and R. Wynands, "Compact atomic clock based on coherent population trapping," *Electron. Lett.*, vol. 37, pp. 1449-1451, 2001.

[2] D. K. Walter and W. Happer, "Spin-Exchange Broadening of Atomic Clock Resonances," *Laser Phys.*, vol. 12, pp. 1182-1187, 2002.

[3] R. F. Lacey, A. L. Helgesson, and J. H. Holloway, "Short-Term Stability of Passive Atomic Frequency Standards," *Proc. IEEE*, vol. 54, pp. 170-176, 1966.

[4] S. Appelt, A. B.-A. Baranga, C. J. Erickson, M. V. Romalis, A. R. Young, and W. Happer, "Theory of spin-exchange optical pumping of He-3 and Xe-129," *Physl Rev. A*, vol. 58, pp. 1412-1439, 1998.

[5] D. K. Walter, W. M. Griffith, and W. Happer, "Magnetic slowing down of spin relaxation due to binary collisions of alkali-metal atoms with buffer-gas atoms," *Phys. Rev. Lett.*, vol. 88, art. no. 093004, 2002.

[6] W. Happer, "Optical-Pumping," *Rev. Mod. Phys.*, vol. 44, pp. 169-249, 1972.

[7] S. Appelt, A. B. Baranga, A. R. Young, and W. Happer, "Light narrowing of rubidium magnetic-resonance lines in high-pressure optical-pumping cells," *Phys. Rev. A*, vol. 59, pp. 2078-2084, 1999.